Biomechanical Patient-Specific Model of the Respiratory System Based on 4D CT Scans and Controlled by Personalized Physiological Compliance

Matthieu Giroux[1], Hamid Ladjal[1(✉)], Michael Beuve[2], and Behzad Shariat[1]

[1] LIRIS - CNRS, UMR 5205, Université de Lyon, Université Lyon 1, Lyon, France
hamid.ladjal@liris.cnrs.fr
[2] IPNL- CNRS, UMR 5822, Université de Lyon, Université Lyon 1, Lyon, France

Abstract. In this paper, we present a dynamic patient-specific model of the respiratory system for a whole respiratory cycle, based on 4D CT scans, personalized physiological compliance (pressure-volume curves), as well as an automatic tuning algorithm to determine lung pressure and diaphragm force parameters. The amplitude of the lung pressure and diaphragm forces are specific, and differs from one patient to another and depends on geometrical and physiological characteristics of the patient. To determine these parameters at different respiratory states and for each patient, an inverse finite element (FE) analysis has been implemented to match the experimental data issued directly from 4D CT images, to the FE simulation results, by minimizing the lungs volume variations. We have evaluated the model accuracy on five selected patients, from DIR-Lab Dataset, with small and large breathing amplitudes, by comparing the FE simulation results on 75 landmarks, at end inspiration (EI), end expiration (EE) states, and at each intermediate respiratory state. We have also evaluated the tumor motion identified in 4D CT scan images and compared it with the trajectory obtained by FE simulation, during one complete breathing cycle. The results demonstrate the good quantitative results of our physic-based model and we believe that our model, despite of others takes into account the challenging problem of the respiratory variabilities.

1 Introduction

Dynamic patient-specific computational modeling and simulation of the respiratory system, is one of the important areas of research in radiation therapy and medical imaging [1]. Tumor motion during irradiation reduces the target coverage and increases dose deposition within healthy tissues. The respiratory motion modifies both the shape and the position of internal organs. Lung tumors can even present hysteresis in their trajectories [2], and generally, it is very difficult or impossible to accurately identify the tumor location during the treatment. This uncertainty on the position makes necessary the development of a strategy for the prediction of tumor motion. One way is to directly image the motion of

M. Descoteaux et al. (Eds.): MICCAI 2017, Part II, LNCS 10434, pp. 216–223, 2017.
DOI: 10.1007/978-3-319-66185-8_25

the tumor and other internal organs during treatment, as done with Cyberknife system. Some lung tumors may be visible using x-ray imaging, but generally it is very difficult to accurately identify the tumor. The other solution is to use implanted markers. However, all these approaches are invasive and would greatly increase the radiation dose to the patient due to imaging. An alternative way is to use a correspondence model to find the relationship between the internal organs motion and the external respiratory surrogate signals, such as spirometry or the displacement of the skin surface, which can be easily measured during treatment [1]. Methods to estimate respiratory organ motions (internal organs) can be divided into two main classes; image registration and biophysical modeling. In image registration, motion fields are directly calculated and extracted from 4D image sequences (CT or IRM) [1], without taking into account knowledge about anatomy and physiology of the respiratory system. In contrast, biophysical (biomechanical) approaches aim at identification and take into account the different anatomical and physiological aspects of breathing dynamics and attempt to describe respiratory-induced organ motion through a partial differential equations (PDEs), based on continuum media mechanics solved frequently by Finite Element Methods (FEM) [3,5,6,9]. Unfortunately, most of the time, the authors have used a single organ (lung) with nonrealistic boundary conditions. Moreover, these simulations are static and do not take into account the dynamic variabilities of the respiratory system and none of these methods consider the real physiological respiratory motion. However, some authors have proposed biomechanical models including the behavior of other organs of the respiratory system (diaphragm, thorax, skin...) coupled with optimization algorithms. In [7] the authors present an ad-hoc evolutionary algorithm designed to explore a search space with 15 dimensions for the respiratory system to estimate the parameters of lung model behavior. Recently, the authors in [4,8] have proposed patient specific biomechanical model of the lung motion from 4D CT images for half respiratory cycle, where the motion is not constrained by any fixed boundary condition. The authors have respectively used 4 and 16 pressure zones on the sub-diaphragm and thoracic cavity. Unfortunately, none of these methods take into account the real physiological respiratory motion. Its control or monitoring by the external parameters could be impossible.

In this paper, we propose an approach to internal movement monitoring with two external parameters, the volume of air exchanged and the thoracic movement (rib kinematics). This model is a 4D dynamic and realistic biomechanical patient-specific model of the respiratory system, constrained by real boundary conditions from the anatomy, based on automatic tuning algorithm to compute lung pressures and diaphragm forces during a whole respiratory cycle. The amplitude of the lung pressure and diaphragm force are patient specific and determined at different respiratory states. In Sect. 2, we present the 3D segmentation and reconstruction, as well as the lung-pressure/diaphragm-force optimization algorithms based on biomechanical model. In Sect. 3, a qualitative and quantitative analysis and experimental validation are presented. Finally, we give some concluding remarks and directions for future work.

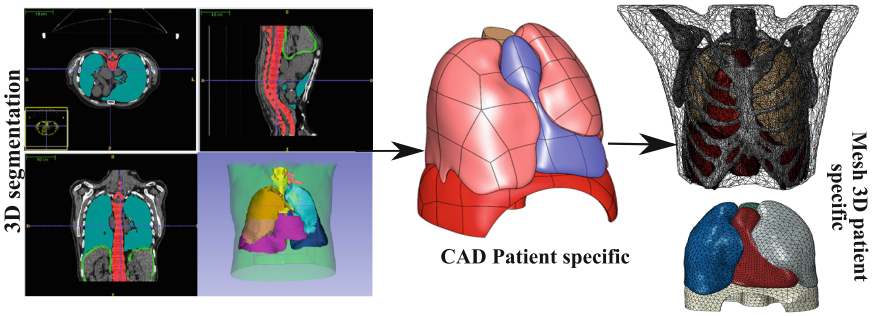

Fig. 1. 3D segmentation, CAD reconstruction and 3D mesh generation for finite element simulations.

2 Materials and Methods

2.1 3D Segmentation and Reconstruction

Various approaches for multi-organ and lung segmentation have been developed based on CT images, which include gray-level threshold, region growing or edge tracking. In this paper, the thorax, the lungs and the external skin are segmented automatically using gray-level threshold algorithms available within ITK-SNAP library[1]. The human diaphragm was segmented manually. To extract the mediastinum structure, we have used the different segmentation masks of the lungs, the thorax, the inner thoracic region and the diaphragm. A Boolean operation between the trunk volume and these masks, permits to reconstruct easily the mediastinum volume. The automatic segmentation of lung tumors remains quite challenging as they are directly in contact with healthy tissues and the different existing methods (automatic or manual) suffer from a lack of reproducibility. Thus, the correct segmentation can only be achieved by medical experts.

After segmentation, a 3D surface mesh is created for each volume, using the marching cubes algorithm. Due to the excessive number of nodes and large number of bad quality elements, which are common features in mesh-based models, a CAD-based approach has been developed. The meshes are rebuilt as a solid using a procedure of semi-automatic surface creation with NURBS. Using the resulting smooth surface, a quality mesh with four-nodes tetrahedral elements is generated using ABAQUS packages (Fig. 1).

2.2 Dynamic Biomechanical Patient-Specific Model of the Respiratory System

The organs are considered as isotropic, elastic, and hyperelastic materials. For an isotropic elastic or hyperelastic material, the elastic energy, noted W, may be written as:

[1] ITK-SNAP is a software application used to segment structures in 3D medical images.

$$W(\mathbf{E}) = \frac{\lambda}{2}(tr\,\mathbf{E})^2 + \mu\,(tr\,\mathbf{E}^2) \tag{1}$$

where $\mathbf{E}$ is the Green-Lagrange strain tensor, λ and μ are the Lame coefficients. The second Piola-Kirchhoff stress tensor and the Green-Lagrange strain tensor given by: $\mathbf{S} = \lambda\,(tr\,\mathbf{E})\,\mathbf{I} + 2\,\mu\,\mathbf{E}$. For dynamic simulation using FEM, the equation of motion of a vertex l of the organ mesh can be written:

$$M^l\{\ddot{\mathbf{u}}_l\} + \gamma^l\{\dot{\mathbf{u}}_l\} + \sum_{\tau \in \mathbf{l}} \left(\{\mathbf{F}_l^{int}\}\right) = \{\mathbf{F}_{ext}^l\} \tag{2}$$

where M^l, γ^l are respectively the mass computed from Hounsfield densities [11] and damping coefficients of each vertex. The V_l is the neighborhood of vertex l (i.e. the tetrahedra containing node l). The $\mathbf{F}_l^{int}$ are the internal forces calculated by FE method and the $\mathbf{F}_{ext}^l$ are the imposed forces calculated by our developed automatic tuning algorithm based on inverse FE. To solve the dynamic system, the implicit finite scheme has been chosen for more stability.

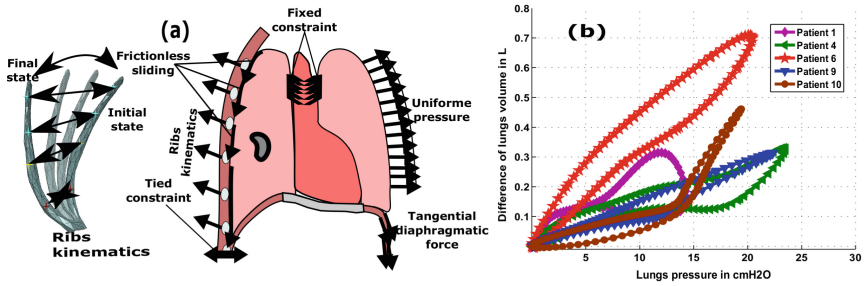

Fig. 2. The boundary conditions (BC) of our patient specific biomechanical model including rib kinematics (a), and the personalized compliance (b).

2.3 The Boundary Conditions (BC)

The boundary conditions (BC) are inferred from the anatomy and identified by medical experts (Fig. 2(a)). For the diaphragm, we have applied the radial direction of muscle forces, which corresponds anatomically to the direction of muscle fibers. The force is applied to the muscular part of the diaphragm and simple homogeneous Dirichlet boundary condition is applied to the lower part of the diaphragm and the Lagrange multiplier's method is used for the contact model. To simulate the sliding of the lungs, a surface-to-surface contact model is applied to the lung-chest cavity. The frictionless contact surfaces are used to simulate the pleural fluid behavior. To simulate the rib cage kinematics, an automatic rigid registration algorithm has been developed from the patients' 4D CT: for each rib, an Euclidean transformation has been computed between EI and EE states. Then we calculated the transformation parameters for each intermediate respiratory state. These parameters have been applied as displacement boundary conditions during the whole respiratory cycle. The originality of our work

compared to the existing works is: (1) The amplitude of the lung pressure and diaphragm force are patient-specific, determined at different respiratory states by an optimization framework based on inverse FE analysis methodology, using lung volume variation. We have segmented the respiratory system at end inspiration (EI, the reference state). Also, we have segmented lungs at 10 states for a full cycle. Then, the model is controlled by a personalized pressure-volume curve (semi-static compliance), calculated by $C_{ss} = \frac{3(1-2\nu)}{E\, V_{t-1}}$ (Fig. 2(b)). The semi-static compliance (C_{ss}) or a specific compliance, based on the tissue properties (Young Modulus E and ν Poisson coefficient) and the lung volume V_t at each step t (respiratory phases) is calculated from 4DCT scan images. For each respiratory volume V_t (from CT scan data), the internal lung pressure is computed. Then by minimizing the lung volume errors, between the V_t and the simulated volume (V_s), the appropriate diaphragm forces are computed. (2)The organs' masses have been computed from the voxelized CT attenuation values. Based on the principal of mass conservation, the masses are distributed on the mesh vertices according to [11]. (3) the developed biomechanical respiratory model is monitored directly by simulated actions of the breathing muscles: the diaphragm and the intercostal muscles (the rib cage). The mechanical properties of the different organs used in our simulations are settled in the (Fig. 3).

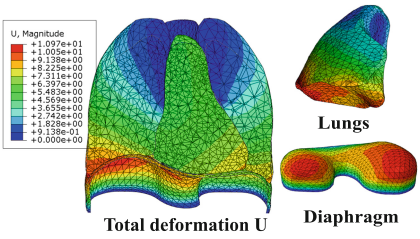

Tissues	Mechanical behavior	E (MPa)	ν	ρ (t/mm^3)
Lungs	HSVK	$3.74\,10^{-3}$	0.3	$3\,10^{-10}$
Lung tumor	LE	49	0.4	1.510^{-9}
Mediastinum	LE	$5.87\,10^{-3}$	0.4	$1\,10^{-10}$
Diaphragm muscle	HSVK	5.32	0.33	$1\,10^{-9}$
Diaphragm tendon	LE	33	0.33	$1\,10^{-9}$
Ribs	LE	5000	0.3	$1.5\,10^{-9}$
Cartilage	LE	49	0.3	$1\,10^{-9}$
Body of sternum	LE	11500	0.3	$1.5\,10^{-9}$
Thoracic vertebra	LE	9860	0.3	$1.5\,10^{-9}$
Flesh	LE	5.32	0.4	$1\,10^{-6}$

Table

Fig. 3. Left: qualitative analysis of patient specific biomechanical simulation; lungs and diaphragm deformations, right (Table) Mechanical properties of breathing system: LE Linear Elastic, HVSK Hyperelastic Saint Venant Kirchhoff, E Young's modulus, ν Poisson coefficient, ρ volumetric density.

3 Results and Experimental Validation

We have evaluated the motion estimation accuracy on five selected patients, from DIR-Lab Dataset [10], with small and large breathing amplitudes (Patient 1 = 10.9 mm, Patient 4 = 18.1 mm, Patient 6 = 27.2 mm, Patient 9 = 15.5 mm and Patient 10 = 26.06 mm). The Fig. 2(b) illustrates the different specific compliances for each patient, calculated and identified at each respiratory state directly

from 4D CT scan images. Then, these compliances are used as input in our biomechanical model to simulate a full respiratory cycle. In our FE simulation, we set the simulation time for the inspiration phase 2 s and for the expiration phase 3 s. The Fig. 3 shows the total deformation and the maximum displacement components of the lungs and diaphragm during breathing. We can observe the maximum displacement of the diaphragm on the right-posterior (RP) and left-posterior (LP) sides. We also notice a slightly larger (RP) side motion than (LP) side motion, in concordance with the physiological anatomy. For the lungs deformation, the results cope with the 4DCT, with the maximum displacement occurring in the posterior region along the superior-inferior (SI) direction. The performance of the proposed biomechanical model has been evaluated by comparing the simulation results with ground truth (CT images) on 75 landmarks available only between EI and EE and intermediate states. However, the tumor trajectory has been evaluated on a full breathing cycle (10 states). The Table 1, shows the comparative study between our FE simulation results and the ground-truth displacement vectors for five patients. In our simulation, we have obtained an average mean error for all ground-truth landmarks: 1.8±1.3, 2.0±1.2, 2.0±1.3, 1.9 ± 1.2 and 1.8 ± 1.3 (mm) respectively for P1, P4, P6, P9 and P10 respectively. These results show that the developed biomechanical model coupled with the personalized lung-pressure/diaphragm-force optimization algorithm of the respiratory system is in a good agreement with the experimental data, and produces more accurate predictions with lower errors than other works [8,9] applied to the same data sets and despite using less parameters.

Table 1. Average landmark lung error (mm) during respirat ion at different respiratory states: the first T00, the end inspiration (T50), the end expiration (T10)

Patients	Mean ± SD (mm)					Mean
	T10	T20	T30	T40	T50	All states
Patient 1	2,1 ± 1,5	2,2 ± 1,2	2,1 ± 1,6	1,6 ± 1,4	1,1 ± 0,8	1,8± 1,3
Patient 4	2,3 ± 1,2	2,5 ± 1,3	2,1 ± 1,2	1,8 ± 1,2	1,5 ± 1,2	2.0± 1.2
Patient 6	2.4 ± 1.5	2.3 ± 1.2	2,0 ± 1.6	1.9 ± 1.6	1.4 ± 1,1	2.0± 1.3
Patient 9	2,3 ± 1,4	2,2 ± 1,1	2,1 ± 1,3	1,8 ± 1,4	1,3 ± 0,9	1.9± 1.2
Patient 10	2,1 ± 1,5	2,2 ± 1,2	2,1 ± 1,6	1.6 ± 1,5	1.1 ± 0.8	1.8± 1.3

The accuracy of our proposed model is illustrated in Table 2, with a mean average error less than (1.9 ± 1.3 mm). Moreover, in order to evaluate the impact of the rib kinematics on lung tumor motion, we have compared the lung tumor trajectories identified in 4D CT scan images with the trajectories estimated by finite element simulation, during the whole breathing cycle (10 phases between the EI and EE). Firstly, to overcome the segmentation difficulties of lung tumor and geometric uncertainties, the affine registration (rigid translation and rotation) method is applied to the lung tumor mesh (with good quality surface reconstruction) at different respiratory states. Then, the accuracy is evaluated on two patients (patient 6 with the tumor location in the left lung, and patient

Table 2. Comparison between our biomechanical patient specific model results and the result s from Vidal et al. [7] and Fuerst et al. [8], on patient 6, patient 9 and patient 10 issued from DIR-Lab Dataset [9].

References	Cycle	Organs Modeled	Boundary conditions	P6 (mm)	P9 (mm)	P10 (mm)
[7] 2012	half	No ribs	4 pressure zones (sub-diaphragm) 16 pressure zones (thoracic)	3.27 ± 1	2.97 ± 1	2.83 ± 1
[8] 2015	half	Only lungs	one CT Uniform pressure	- -	3.2± 1.4	4.4± 2.9
Our model	Full 2s inhalation 3s exhalation	All organs Thorax Diaphragm	Patient specific P-V Rib Kinematics Tangential force	2.0± 1.3	1.9± 1.2	1.8± 1.3

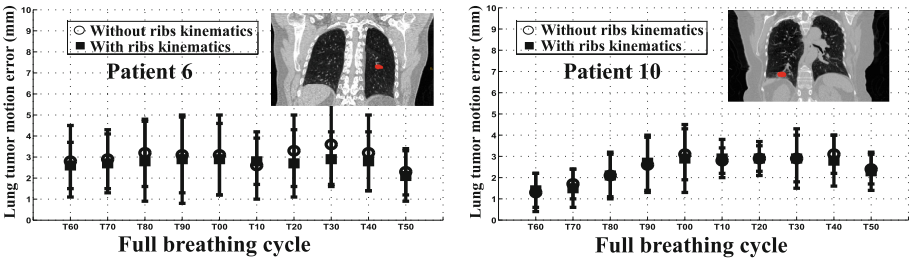

Fig. 4. Mean errors ± standard deviation of lung tumor position during the whole cycle of breathing (10 phases between the EI and EE) between the trajectory issued from 4D CT images compared to the trajectory calculated by biomechanical finite element simulation coupled with the lung-pressure/diaphragm-force optimization for two patients P6 and P10.

10 with tumor in the right lung in contact with the diaphragm), by comparing and calculating the average Hausdorff distance between the 3D mesh surface of the segmented tumor and predicted FE lung tumor, including or not the rib kinematics. Again, the Fig. 4 demonstrates that our patient specific biomechanical model for lung tumor position estimation is very accurate (less than 3 mm). It is important to note that the results are slightly better with the rib kinematics but the difference is not significant during the whole cycle for patient 6 and 10. This is because the respiration for these patients is mainly diaphragmatic.

4 Conclusion

We have developed an accurate dynamic patient specific biomechanical model of the respiratory system for a whole respiratory cycle, based on specific pressure-volume curves, chest movement, as well as an automatic tuning algorithm to

determine specific lung pressure and diaphragm force parameters. The preliminary results are quite realistic compared to the 4DCT scan images. We can observe that the proposed physically based FE model is able to predict correctly the respiratory motion. Currently, we are working on optimization of our patient-specific model to find interactively the correlation between the internal organs motion and the external respiratory surrogate signals, such as spirometry or the displacement of the skin surface during treatment. We believe this could be a potential tool to obtain a valuable tumor motion tracking system, during treatment and to provide medical physicians with necessary information to reduce the margins between clinical target volume (CTV) and planning target volume (PTV).

Acknowledgement. This research is supported by the LABEX PRIMES (ANR-11-LABX-0063), within the program Investissements dAvenir(ANR-11-IDEX- 0007) operated by the French National Research Agency (ANR) and by France Hadron.

References

1. Ehrhardt, J., Lorenz, C.: 4D Modeling and Estimation of Respiratory Motion for Radiation Therapy. Springer, Heidelberg (2013). ISBN 978-3-642-36441-9
2. Seppenwoolde, Y., et al.: Precise and real time measurement of 3D tumor motion in lung due to breathing and heartbeat, measured during radiotherapy. Int. J. Radiat. Oncol. Biol. Phys. **53**, 822–834 (2002)
3. Behr, M., Peres, J., Liari, M., Godio, Y., Jammes, Y., Brunet, C.: A three-dimensional human trunk model for the analysis of respiratory mechanics. J. Biomech. Eng. **132**, 014501-1–014501-4 (2010)
4. Fuerst, B., et al.: A personalized biomechanical model for respiratory motion prediction. In: Ayache, N., Delingette, H., Golland, P., Mori, K. (eds.) MICCAI 2012. LNCS, vol. 7512, pp. 566–573. Springer, Heidelberg (2012). doi:10.1007/978-3-642-33454-2_70
5. AlMayah, A., Moseley, J., Velec, M., Brock, K.: Toward efficient biomechanical-based deformable image registration of lungs for imageguided radiotherapy. Phys. Med. Biol. **56**(15), 4701 (2011)
6. Ladjal. et al. B, Biomechanical Modeling of the Respiratory System: Human Diaphragm and Thorax, Computational Biomechanics for Medicine New Approaches and New Applications, pp. 101–115 (2015)
7. Vidal, F., Villard, P.-F., Lutton, E.: Tuning of patient specific deformable models using an adaptive evolutionary optimization strategy. IEEE Trans. Biomed. Eng. **59**(10), 2942–2949 (2012)
8. Fuerst, B., et al.: Patient-specific biomechanical model for the prediction of lung motion from 4D CT images. IEEE Trans. Med. Imaging **34**(2), 599–607 (2015)
9. Li, F., Porikli, F.: Biomechanical model-based 4DCT simulation. Comput. Methods Biomech. Biomed. Eng.: Imaging Vis. **3**, 222–233 (2015)
10. Castillo, E., et al.: Four-dimensional deformable image registration using trajectory modeling. Phys. Med. Biol. **55**, 305–327 (2009)
11. Manescu, P., Ladjal, H., Azencot, J., Beuve, M., Testa, E., Shariat, B.: Four-dimensional radiotherapeutic dose calculation using biomechanical respiratory motion description. In: IJCARS, pp. 1–9 (2013)